Earth Planets Space, **58**, 943–949, 2006

Correlation between gravity and magnetic anomalies of Western Anatolia and its relation to tectonic structures

Z. Düzgit, Z. M. Hisarli, N. Sayin, and N. Orbay

İstanbul Üniversitesi, Mühendislik Fakültesi, Jeofizik Mühendisliği Bölümü, Avcılar, Istanbul, Turkey

(Received May 26, 2005; Revised May 5, 2006; Accepted June 9, 2006; Online published September 16, 2006)

In this paper, we apply for the first time the moving-windows application of the Poisson's theorem to the synthetic gravity and magnetic data, followed by calculations of the correlations of the Bouguer gravity and aeromagnetic data of Western Anatolia. The correlation coefficient, slope and intercept parameters were generated from the internal correlations existing between the gravity and magnetic anomalies. Relative negative correlation values of positive gravity and negative magnetic anomalies were found on the Menderes Massif and in the southern part of the Marmara sea. Higher heat flow values were also obtained from these regions. The negative correlation values can be seen on a profile taken along the 28°E longitude and are sourced from a large graben system which has been generated as a result of lithospheric extension in Western Anatolia since the Early Miocene. The grabens were filled up by approximately 2000-m-thick sediments. The negative correlation coefficients and high heat flow values correspond to relative uplift of the asthenosphere in these regions.

Key words: Poisson's theorem, gravity, magnetic, tectonic structures, Western Anatolia.

1. Introduction

With the help of Poisson's theorem, the relation between magnetic and gravitational potentials due to the same source having uniform density and magnetization contrast can be given free from the shape and position of the source. Poisson's theorem has been applied in various methods to several analyses including, for example, the determination of anomaly source magnetization to density ratios (Garland, 1951; Kanasewich and Agarval, 1970) and of the direction of source magnetization (Ross and Lavin, 1966; Cordell and Taylor, 1971). The correlation of potential field data sets including the anomalies has generally been made by visual fitting without using any equation. Chandler *et al.* (1981), however, suggested a new method of analysis based on the Poisson's theorem for calculating the correlation of the gravity and magnetic anomalies.

Poisson's theorem was developed by considering the anomalies within a data set generated from a single source. Only one correlation values set was calculated by using this relationship between the gravity and magnetic data for the region under consideration. Chandler *et al.* (1981) applied the Poisson's theorem to divided regions by using the moving windows method. Accordingly, they calculated a number of correlation values for the area under study instead of only one. Chandler *et al.* (1981) first applied this method to synthetic models, but they subsequently obtained successful results when they applied the methods to the gravity and magnetic anomalies in and around Michigan and Lake City. von Frese *et al.* (1982) also calculated the correlations using Poisson's theorem through the application of the moving window method to the gravity and magnetic data of North America. In their study an inverse relationship was observed between long-wavelength gravity and magnetic anomalies over the continental terrain. The areas of negative gravity and positive magnetic anomalies were found to be characterized by relatively thick crust and high magnetization, whereas the negative magnetic and positive gravity anomalies were characterized by a thinner crust and higher heat flow.

Akdoğan (2000) correlated the gravity, magnetic and heat flow anomalies for a region located between 38° and 40°N and 26° and 30°E in Turkey and found that positive magnetic and high negative gravity anomalies were correlated with thick acidic and basic intrusive rocks.

This study aims at providing an understanding of the crustal and thermal structure of Western Anatolia by taking the tectonic structure into account. The method of Chandler *et al.* (1981) was first applied to the synthetic models. The correlation coefficients, slope and intercept values of the Bouguer gravity and aeromagnetic data of the Western Anatolia were then calculated, and these are discussed with special attention to geological and geothermal structure.

2. Method and Application to the Synthetic Data

The relationship between gravitational (U) and magnetic (V) potentials arising from a common, isolated source was shown by Poisson to be

$$V = \frac{1}{G}\frac{\Delta J}{\Delta\sigma}\frac{\partial U}{\partial i} \tag{1}$$

where ΔJ=anomalous source magnetization, $\Delta\sigma$=anomalous source density, i=direction of source magnetization and G=universal gravitational constant. For this simple linear relationship to be valid, the isolated source must have a

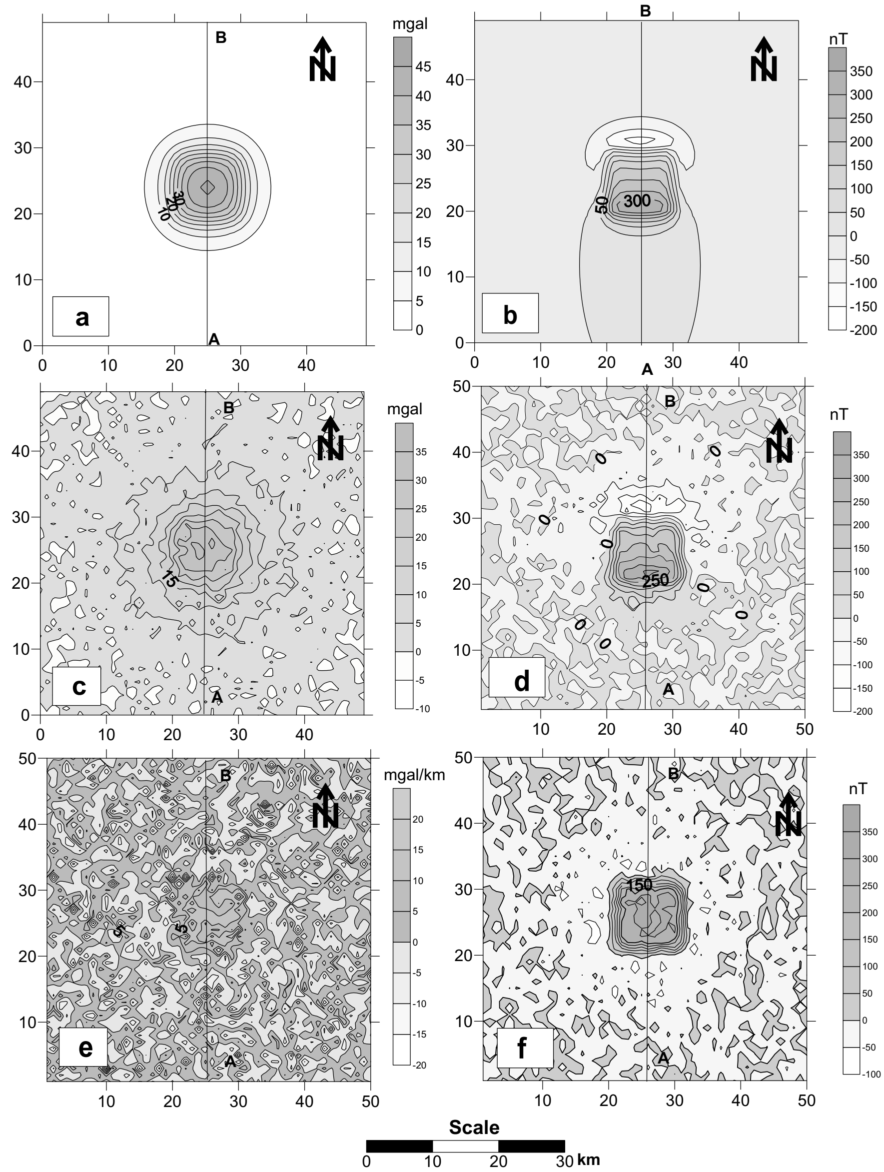

Fig. 1. The gravity and magnetic anomalies calculated using the parameters given in Table 1 (a and b). The contaminated synthetic gravity and magnetic anomalies (c and d). The vertical derivative of the gravity and magnetic anomaly reduced to the pole (e and f).

Table 1. The parameters of the single prism model.

Depth of the top (km)	0
Depth of the bottom (km)	5
Width on the x direction (km)	10
Width on the y direction (km)	10
Density contrast (gr/cm^3)	0.1
Declination of the magnetization of the prism	0°
Inclination of the magnetization of the prism	60°
Declination of the earth's magnetic field	0°
Inclination of the earth's magnetic field	60°
Susceptibility of the prism (cgsemu)	0.001
$\Delta J/\Delta\sigma$	0.002

uniform density and magnetization contrasts. This relationship, however, is independent of the shape and position of the source.

Poisson's theorem can be modified to express the relationship between the total magnetic intensity anomaly reduced to the pole (T_z) and the gravity anomaly (g)

$$T_z = \frac{1}{G}\frac{\Delta J}{\Delta\sigma}\frac{\partial g}{\partial z} \quad (2)$$

where $\partial g/\partial z$ is the first order vertical derivative of the gravity anomaly. Equation (2) can be written as

$$T_z = A + \frac{1}{G}\frac{\Delta J}{\Delta\sigma}\frac{\partial g}{\partial z} \quad (3)$$

if regional-scale anomalies are taken into consideration. "A" is the intercept coefficient which gives the anomaly base-level for the data within the window intercept coefficient caused by long-wavelength anomaly components.

By substituting B and X instead of $(\Delta J/\Delta\sigma)$ and $(1/G)(\partial g/\partial z)$, respectively, in Eq. (3), we get a linear equation as

$$T_z = A + BX \quad (4)$$

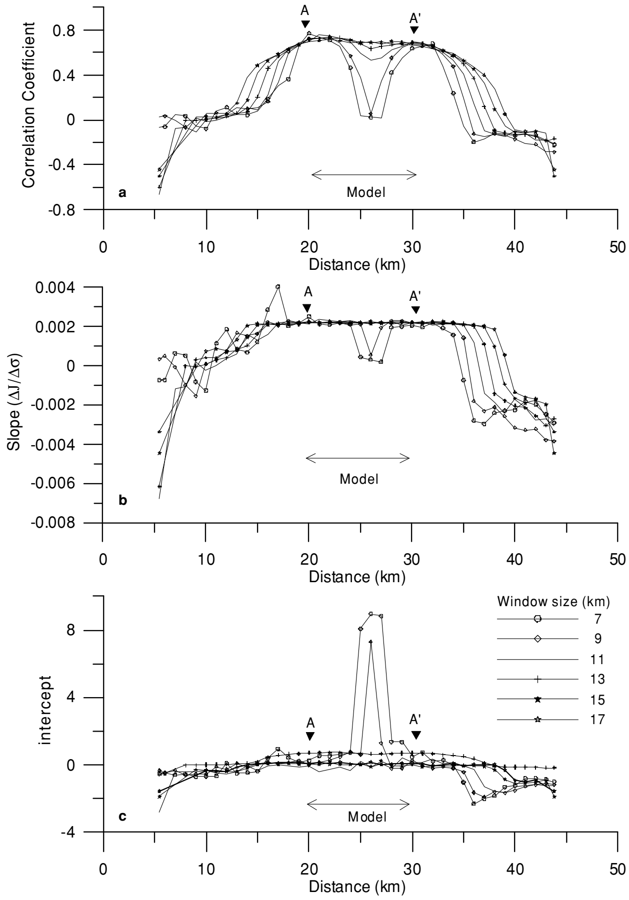

Fig. 2. Correlation coefficients (a), slope ($\Delta J/\Delta\sigma$) (b) and intercept (c) values were calculated from contaminated gravity and magnetic data obtained using different lengths of windows, such as 7, 9, 11, 13, 15 and 17 km.

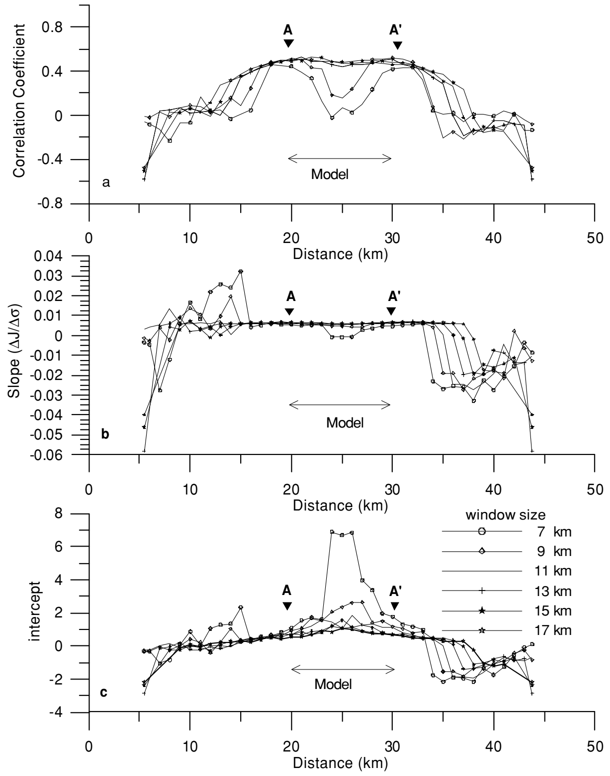

Fig. 3. Correlation coefficients (a), slope ($\Delta J/\Delta\sigma$) (b) and intercept (c) values were calculated from contaminated gravity and magnetic data obtained from two vertically superimposed prisms using different lengths of windows, such as 7, 9, 11, 13, 15 and 17 km.

Table 2. The parameters of the two superimposed prisms model.

	First prism	Second prism
Depth of the top (km)	0	5
Depth of the bottom (km)	5	10
Width on the x direction (km)	10	10
Width on the y direction (km)	10	10
Density contrast (gr/cm^3)	0.1	0.5
Declination of the magnetization of the prism	0°	0°
Inclination of the magnetization of the prism	60°	60°
Declination of the earth's magnetic field	0°	0°
Inclination of the earth's magnetic field	60°	60°
Susceptibility of the prism (cgsemu)	0.001	0.001

where A is the intercept and B the slope value of the correlation between the gravity and magnetic anomalies. The correlation values can be obtained by using a moving-window Poisson's analysis for multi-source gravity and magnetic data set (Chandler *et al.*, 1981).

A single rectangular prism and superimposed rectangular prisms were taken for testing the method by using synthetic data. Parameters of the models are given in Table 1 and 2, respectively. The direction of magnetization of the models is assumed to be that of the earth's magnetic field. The sampling interval of the data is taken as 1 km.

2.1 Single rectangular prism

The gravity and magnetic anomalies of the model that were calculated using the parameters presented in Table 1 are given in Fig. 1(a) and (b). In the subsequent test to derive information on the size of the source, the gravity and magnetic anomalies of this model are contaminated by 5% and 6.5% Gaussian noises which have the standard deviations as 0.19 mgal and 1.09 nT, respectively. The contaminated synthetic gravity and the magnetic anomalies are given in Fig. 1(c) and (d). The vertical derivative of the gravity and magnetic intensity anomaly reduced to the pole by using the contaminated data are given in Fig. 1(e) and (f). These values reduced to the pole and first derivatives are calculated numerically using the PF software of the United States Geological Survey (USGS; http://pubs.usgs.gov/ts/fs-0076-95/FS076-95.html), assuming that the synthetic magnetic data has the same direction as the earth's magnetic field.

The correlation coefficient, slope ($\Delta J/\Delta\sigma$) and intercept values were calculated to obtain the relationship between contaminated gravity and magnetic data using different lengths of windows, such as 7, 9, 11, 13, 15 and 17 km. The calculated variations in the parameters for each length of window are given in Fig. 2(a)–(c) along the AB profile (see Fig. 1 for the location of the profile). The value of the correlation coefficient was suitably approximated to 0.8 when the length of the window was taken as 17 km at the center of the model mass; otherwise, it remained well below 1 (Fig. 2(a)). The value of the ($\Delta J/\Delta\sigma$) ratio in the model is taken as 0.002 cgsemu. This value was obtained

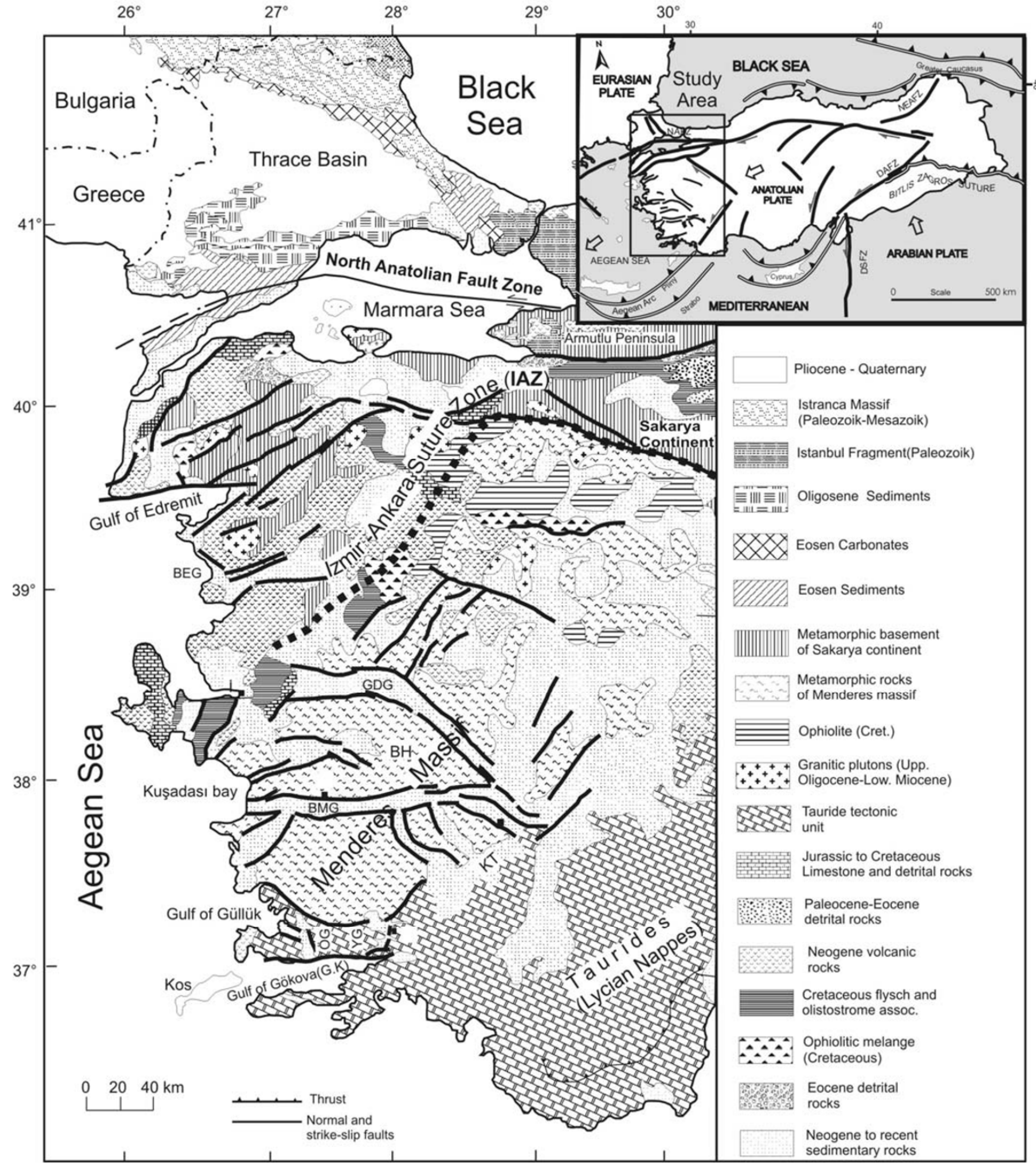

Fig. 4. The geological units and tectonic structures of the study area (modified from Turgut and Eseller, 2000; Yılmaz *et al.*, 2000; Elmas and Gürer, 2004). BEG: Bergama graben, BH: Bozdağ horst, BMG: Büyük Menderes graben, KT: Kale-Tavas Basin, OG: Ören graben, YG: Yatağan graben.

as zero around the center of the mass using 7 and 9 lengths of windows. However, the $(\Delta J/\Delta\sigma)$ ratio is calculated as being very close to 0.002 cgsemu by using other window lengths.

2.2 Two Vertically superimposed rectangular prisms

The vertical superimposed rectangular prism is 10×10 km in cross-section. The top of the upper source is at a depth of 0.1 km, while that of the lower source is at a depth of 5 km. The density contrasts for upper and lower sources are 0.1 and 0.5 cgs, respectively (Table 2). The magnetization contrast of each prism is taken 0.001 cgsemu.

The gravity and magnetic anomalies of this model are both contaminated by 3% Gaussian noises which have standard deviations of 0.1 mgal and 1.78 nT, respectively. The correlation coefficient, slope $(\Delta J/\Delta\sigma)$ and intercept profiles (Fig. 3(a)–(c)) were obtained for above-mentioned window lengths from the vertical derivative of the gravity and magnetic intensity anomalies reduced to the pole.

2.3 Window length selection

The relationship between window length and model parameters are clearly seen in Figs. 2(a)–(c) and 3(a)–(c). According to these figures, the correlation coefficient, slope and intercept values exhibit sudden changes at the center of the model when the window length has a small value such as 7 or 9. The maximum points of these variations (the AA′ points in Figs. 2 and 3) show very good fit with the boundaries of the model. The above-mentioned variations disappear when the window length has a relatively larger value such as 13, 15 and 17.

In conclusion, the large window length can provide general features about the structures.

A length smaller than the width of the structures must be selected when the aim is to designate the boundaries of the structures.

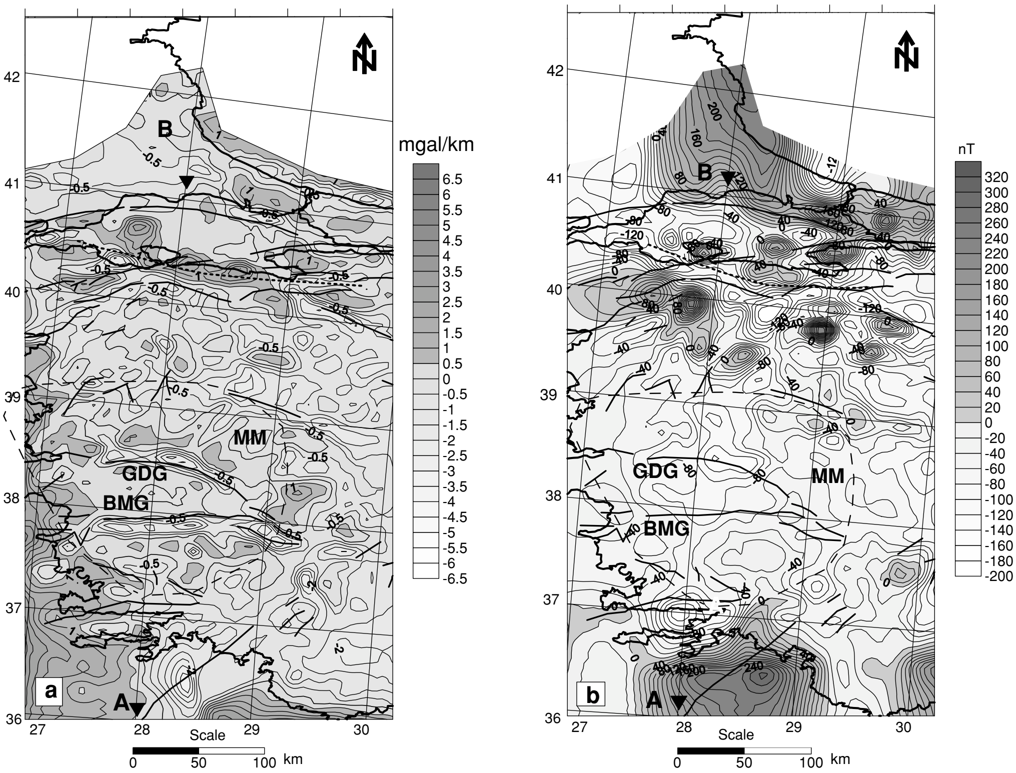

Fig. 5. The first order vertical derivative of the Bouguer gravity anomaly map (a) and the aeromagnetic anomaly map reduced to the pole (b) of Western Anatolia. The Menderes massif is outlined by dashed lines in both figures. BMG: Büyük Menderes graben, GDG: Gediz graben, MM: Menderes massif. The solid lines show the observed main faults in Western Anatolia.

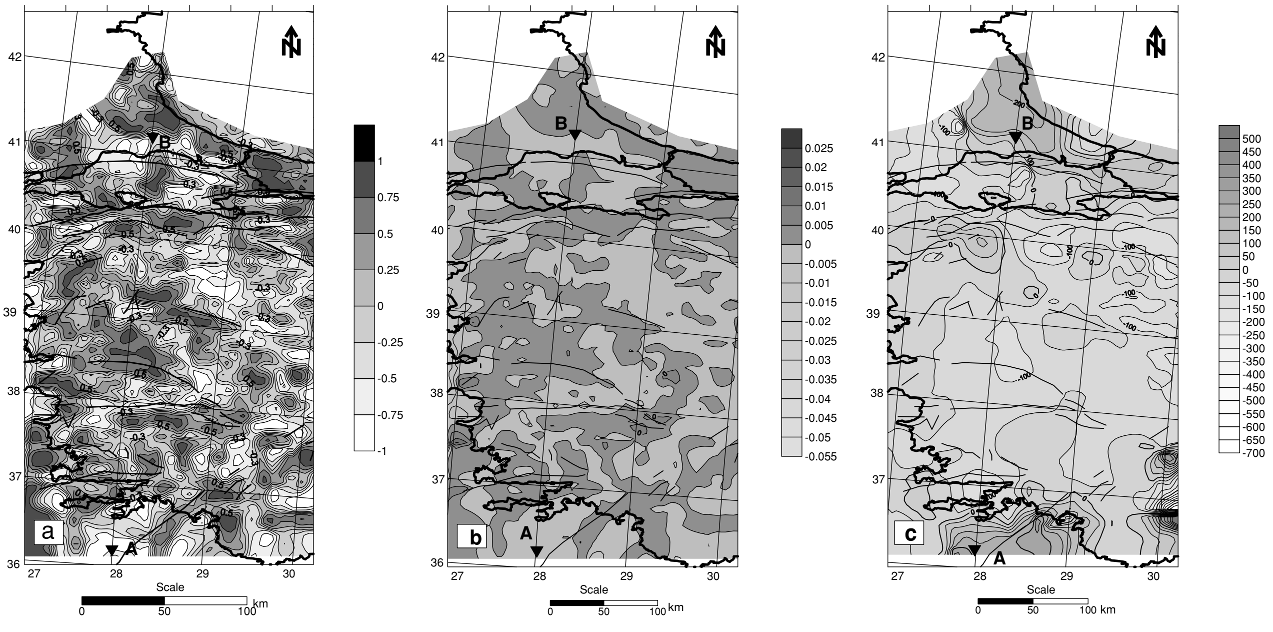

Fig. 6. The correlation coefficients (a), slope (b) and intercept (c) values obtained from the linear relationship application of the Poisson's Theorem to the first order vertical derivative of the Bouguer anomaly and aeromagnetic data reduced to the pole. The solid lines show the observed main faults in the Western Anatolia.

3. Application to the Gravity and Aeromagnetic Data of Western Anatolia

The area under study is approximately between 36° and 41.5°N and 27° and 30°E in Turkey. The geological units and tectonic structures are shown in Fig. 4. The Bouguer gravity map was prepared by the Mineral Research Institute of Turkey, while the magnetic anomaly map was obtained after removing the main field using the algorithm of Malin and Barraclough (1981). The data are projected on a plane using the Albers projection. Before the application of Poisson's theorem to the gravity and magnetic data, upward continuation to 5 km was applied to the Bouguer

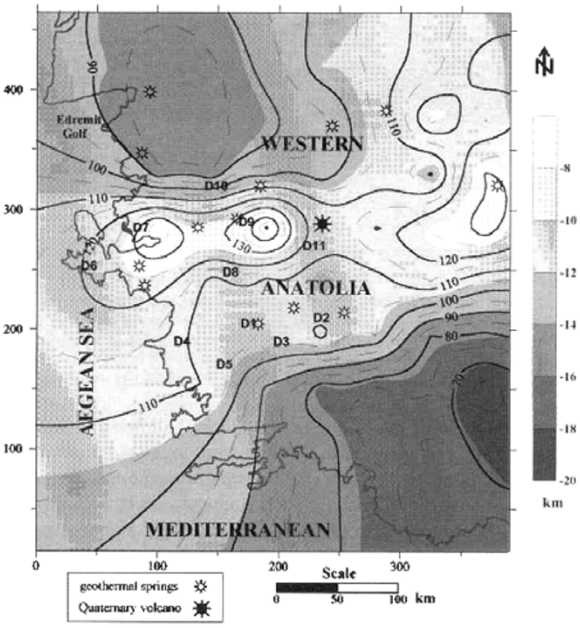

Fig. 7. Curie point depths and heat flow map of Western Anatolia (Dolmaz *et al.*, 2005).

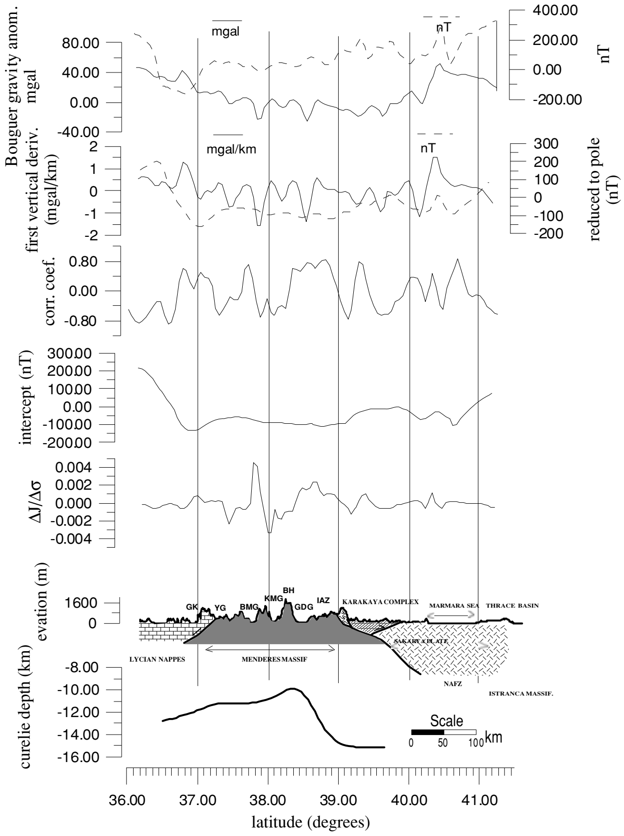

Fig. 8. Bouguer gravity and aeromagnetic anomalies and their first order vertical derivative and reduced to the pole profiles, general characteristics of the correlation values, exemplified profile of the faults and graben and horst structures and Curie depths profiles. BH: Bozdağ horst, BMG: Büyük Menderes graben, GK: Gulf of Gökova, GDG: Gediz graben, IAZ: İzmir-Ankara suture zone, KMG: Küçük Menderes graben, NAFZ: North Anatolian Fault Zone, YG: Yatağan graben.

gravity and aeromagnetic data to obtain the regional effects of large and deeper geological masses. First order vertical derivatives were then taken (Fig. 5(a)). Reduction to the pole process was applied to the upward projecting aeromagnetic data, which were obtained by removing the main field value of 1982. This map is given in Fig. 5(b).

Determination of the length of the window is important when the correlation coefficient, slope and intercept values between gravity and magnetic data have been obtained using Poisson's theorem. The width of the grabens in Western Anatolia changes between 2 and 20 km. However, there are also great geological structures which are covered by large areas, such as the Menderes Massif (this massif is indicated by dashed lines in Fig. 5(a) and (b)). For this reason we decided to obtain a window size that was sevenfold larger than the sampling interval of the data. When the sampling interval is taken as 5 km, the window size will be 35 km, so it is possible to see the effect of graben structures on the correlation values between the gravity and magnetic anomalies.

The correlation coefficients, slope and intercept values obtained from the linear relationship of Eq. (3) with the moving window applied to the first order vertical derivative of Bouguer anomaly and aeromagnetic data reduced to the pole are given in Fig. 6(a), (b) and (c), respectively. The main faults in Western Anatolia are also shown in these figures.

The southern part of the Marmara Sea is characterized by aligned positive gravity and negative magnetic anomalies when we compare the first order vertical derivative gravity anomaly dotted lines on Fig. 5(a) and the magnetic maps reduced to the pole dotted lines on Fig. 5(b). Pfister *et al.* (1998) obtained heat flows ranging from 35 to 115 mW/m^2 at the southern part of the Marmara Sea and suggested that the extensional tectonic regime of the region was characterized by high heat flow values. The Curie point depths and heat flow map obtained by Dolmaz *et al.* (2005) is given in Fig. 7. Heat flow values vary between 110 and 130 mW/m^2 on the Menderes Massif. Positive gravity and negative magnetic anomalies and high heat flow values on and around the Menderes Massif suggests that the asthenosphere is uplifted in this region.

The correlation coefficients and slope values ($\Delta J/\Delta\sigma$) which are illustrated in Fig. 6(a) and (b) show very good agreement with the boundary of the geological structures in Western Anatolia. For example, the correlation coefficient obtained on the Menderes Massif, which is situated between 38° and 39°N and 27.5° and 28.5°E, is almost +0.8, while this coefficient is calculated to be −0.8 on the sedimentary structure of the Menderes Massif. The slope ($\Delta J/\Delta\sigma$) values, which generally vary between +0.005 and −0.005, are related to the kind of the geological formations. The magnetic anomalies have quite low intensities while positive and negative gravity anomalies are seen below the latitude of 38°N (see Fig. 5 (a) and (b)). Therefore, the slope variations are most likely to depend on the density contrast. The surrounding area of the Menderes Massif shows a negative correlation associated with decreasing magnetic and increasing positive gravity anomalies. This may result from the presence of thick sedimentary grabens formed under the effect of extensional tectonic regime.

The general characteristics of the correlation parameters of the Bouguer gravity and the aeromagnetic anomalies are clearly exemplified by a profile that is crossing the faults, grabens and horsts along the 28°E longitude, as illustrated in Fig. 8. The Bouguer gravity and magnetic anomalies, magnetic anomalies reduced to the pole, first order vertical derivative of the gravity anomalies, correlation coefficients, variation of the intercept and slope values, simplified geological cross section and Curie depth profile are shown in this figure.

Several characteristic features of these values correspond to the underground geology as follows:

(1) The variation in the correlation coefficients illustrates inverse correlations on the Menderes Massif and in the southern part of the Marmara Sea. This negative correlation may be related to the presence of a relatively thick crust and high heat flows, as stated above.

(2) The Lycian nappes and the Menderes Massif consist mainly of sedimentary and metamorphic rocks, respectively, which have small magnetization and high density contrasts.

(3) The fluctuation on the slope variation around 38°N latitude corresponds to highly magnetized granitic plutons intruding into the metamorphic rocks of the Menderes Massif.

(4) The variations in correlation coefficients, intercept and slope fluctuations on the 39.5° and 41°N latitudes show very good similarity with the shape of moving-window regression parameters for two vertically superimposed sources, as shown in Fig. 3. These variations on the correlation coefficients and the others could be related with the boundaries of the Karakaya complex and Sakarya continent, as mentioned in the section on the selection of the lengths of the windows.

(5) The Sakarya plate is placed approximately between 39.5° and 41.5°N in Fig. 8. The Thrace Basin and the Karakaya complex, including volcanic, metamorphic and sedimentary rocks, are placed in the northern and southern parts of the Sakarya Continent, respectively. The Marmara Sea Basin, filled by 2-km-thick sediments, is situated between the Thrace Basin and the Sakarya plate. The gneiss-amphibolite basement of the Sakarya Continent is also present beneath the Thrace and Marmara Sea Basins. The obtained shape of the regression parameters over two different structures, such as the gneiss-amphibolites basement and its sedimentary cover, shows very good agreement with the calculated model of two vertically superimposed sources.

(6) Small slope values are obtained for the Marmara Sea (Fig. 6 (b)). In our opinion these small slope variation values on the Marmara Sea could be related to the North Anatolian Fault Zone.

4. Conclusion

Regression parameters of gravity and magnetic anomalies over Western Anatolia were calculated, satisfying the theoretical considerations of Poisson's theorem in regions of common potential field sources. The obtained correlation coefficient map indicates either positive or negative values related to the geological formations and geothermal areas, such as the southern part of Marmara Sea, over and around the Menderes Massif and over the graben structures of Western Anatolia.

Two different structures, such as gneiss and amphibolites, beneath the Karakaya complex and Thrace Basin show similarities with the calculated model of two vertically superimposed sources. The variations in the correlation coefficients, slope and intercept values could also be related with the boundaries of such structures as the Karakaya complex, Sakarya continent and Istranca massif.

Acknowledgments. The authors thank the General Directorate of Mineral Research and Exploration (MTA) for providing Bouguer gravity and aeromagnetic maps. We also thank Dr. Timur Ustaömer and Dr. Demir Kolçak for valuable comments. We acknowledge valuable suggestions and reviews by Dr. Yoichi Sasai and Dr. Tadashi Nakatsuka. We are grateful to the editor Dr. Makoto Uyeshima. This work was supported by the Istanbul University Research Found, Project no: 1488/28072000.

References

Akdoğan, N., İzmir paftası gravimetrik-manyetik-ısı akısı anomalilerinin jeolojik korelasyonu ve bazı sonuçlar, Batı Anadolu'nun Depremselliği Sempozyumu, Bildiriler kitabı 507–508, 2000, İzmir.

Chandler, V. W., J. S. Koski, W. J. Hinze, and L. W. Braile, Analysis of multisource gravity and magnetic anomaly data sets by moving-window application of Poisson's Theorem, *Geophysics*, **46**, 30–39, 1981.

Cordell, L. and P. T. Taylor, Investigation of magnetization and density of North Atlantic Seamount using Poisson's Theorem, *Geophysics*, **36**, 919–937, 1971.

Dolmaz, M. N., Z. M. Hisarlı, T. Ustaömer, and N. Orbay, Curie point depths based on spectrum analysis of aeromagnetic data, West Anatolian Extentional Province, Turkey, *Pure Appl. Geophys.*, **162**, 571–590, 2005.

Elmas, A. and A. Gürer, A comparison of the geological and geoelectrical structures in the Eastern Marmara region (NW Turkey), *J. Asian Earth Sci.*, 153–162, 2004.

Garland, G. D., Combined analysis of gravity and magnetic anomalies, *Geophysics*, **16**, 51–62, 1951.

Kanasewich, E. R. and R. G. Agarwal, Analysis of combined gravity and magnetic fields in wave number domain, *J. Geophys. Res.*, **75**, 5702–5712, 1970.

Malin, S. R. C. and D. R. Barraclough, An algorithm for synthesing the geomagnetic field, *Computers Geosci.*, **7**, 401–405, 1981.

Pfister, M., L. Rybach, and Ş. Şimşek, Geothermal reconnaissance of the Marmara Sea region (NW Turkey): surface heat flow density in an area of active continental extension, *Tectonophysics*, **291**, 77–89, 1998.

Ross, H. P. and P. M. Lavin, In-situ determination of the remanent magnetic vector of two-dimensional tabular bodies, *Geophysics*, **31**, 949–962, 1966.

Turgut, S. and G. Eseller, Sequence stratigraphy, tectonics and depositional history in eastern Thrace Basin, NW Turkey, *Mar. Petrol. Geol.*, **7**, 61–100, 2000.

von Frese, R. R. B., W. J. Hinze, and L. W. Braile, Regional North American gravity and magnetic anomaly correlations, *Geophys. J. R. Astr. Soc.*, **69**, 745–761, 1982.

Yılmaz, Y., Ş. C. Genç, Ö. F. Gürer, M. Bozcu, K. Yılmaz, Z. Karacık, Ş. Altunkaynak, and A. Elmas, When did the Western Anatolian grabens begin to develop, in *Tectonics and Magmatism in Turkey and the Surrounding Area*, edited by E. Bozkurt, J. A. Winchester, and J. D. A. Piper, Geol. Soc. London, **173**, 353–384, 2000.

Z. Düzgit (e-mail: zduzgit@istanbul.edu.tr), Z. M. Hisarli, N. Sayin, and N. Orbay